Flexibility of Liver Alcohol Dehydrogenase in Stereoselective Binding of 3-Butylthiolane 1-Oxides[†,‡]

Heeyeong Cho,[§] S. Ramaswamy,[||] and Bryce V. Plapp*[,§]

Department of Biochemistry, The University of Iowa, Iowa City, Iowa 52242, and Department of Molecular Biology, Swedish University of Agricultural Sciences, Biomedical Center, Box 590, S-751 24 Uppsala, Sweden

Received September 29, 1996; Revised Manuscript Received November 12, 1996[⊗]

ABSTRACT: Thiolane 1-oxides are analogs of the carbonyl substrates that bind to the alcohol dehydrogenase−NADH complex and are potent uncompetitive inhibitors against alcohol [Chadha, V. K., et al. (1985) *J. Med. Chem. 28*, 36−40]. The four stereoisomers of 3-butylthiolane 1-oxide (BTO) were separated by chiral phase chromatography. CD and ^{1}H-NMR spectra identified the enantiomeric pairs. ^{1}H-NMR chemical shifts were assigned on the basis of COSY spectra of both diastereoisomers and confirmed by HMQC spectra. Coupling constants were determined through one-dimensional decoupling experiments. NMR with chiral shift reagents, Eu(hfc)$_3$ [europium tris[3-[(heptafluoropropyl)hydroxymethylene]-(+)-camphorate]] or (*R*)-(−)-*N*-(3,5-dinitrobenzoyl)-α-methylbenzylamine, determined that the most inhibitory isomer is either 1*S*,3*R* or 1*R*,3*S*. The chemical shifts of protons in the thiolane 1-oxide ring were influenced by the whole structure and were not correlated with the computed Mulliken charges. X-ray crystallography at 2.1 and 1.66 Å resolution of the ternary enzyme complexes with NADH demonstrated that the absolute configuration of the most inhibitory (K_{ii} = 0.31 μM) stereoisomer is 1*S*,3*R* and the next best inhibitor (K_{ii} = 0.73 μM) is 1*S*,3*S*. The thiolane 1-oxide rings bind in the same position, in the substrate binding site, but the geometry of the complexes suggests that the sulfoxides are not transition state analogs. Significantly, the butyl groups of the two isomers are accommodated differently by flexible amino acid side chains adopting alternative rotameric conformations.

Liver alcohol dehydrogenase (ADH,[1] EC 1.1.1.1) is a major rate-limiting enzyme for metabolism of ethanol; however, the enzyme has broad substrate specificity, and its physiological roles are uncertain (Plapp, 1975; Plapp et al., 1984). Inhibitors can be used to map the topology of the active site and could be used to prevent the oxidation of methanol and ethylene glycol to their toxic acids (Theorell et al., 1972; Chen et al., 1981; Plapp, 1994). 4-Methylpyrazole is a potent inhibitor of ADH and may be useful as a therapeutic agent (Blomstrand et al., 1980). However, it is competitive against alcohol so that high concentrations of alcohol reverse the inhibition, which is in contrast to uncompetitive inhibitors that remain effective (Chadha et al., 1983).

3-Substituted derivatives of thiolane 1-oxide are unusually potent uncompetitive inhibitors, which bind to the enzyme−NADH complex and could be transition state analogs (Chadha et al., 1985). They have two chiral centers, at S1 and C3, on the five-membered ring and consequently four stereoisomers. Since the hydrophobic substrate binding pocket of the enzyme is chiral, one of these four stereoisomers would bind most tightly to the enzyme and should be most efficacious. The isomers of the most potent uncompetitive inhibitor *in vivo*, 3-butylthiolane 1-oxide (BTO, Chart 1), were separated, and their configurations were determined by NMR and X-ray crystallography. The X-ray results show how a flexible enzyme binds similar ligands in different ways.

Chart 1: 3-Butylthiolane 1-Oxide

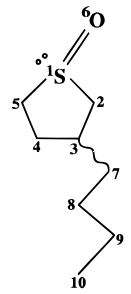

EXPERIMENTAL PROCEDURES

Materials. Crystalline horse liver ADH (EE isoenzyme), NAD$^+$, and NADH were purchased from Boehringer Mannheim. 3-Butylthiolane 1-oxide was synthesized (Chadha et al., 1985). Solvents for HPLC were obtained from Fisher Scientific. $CDCl_3$ was purchased from Isotec. Chiral shift reagents Eu(hfc)$_3$ [europium tris[3-[(heptafluoropropyl)-hydroxymethylene]-(+)-camphorate]] and (*R*)-(−)-*N*-(3,5-dinitrobenzoyl)-α-methylbenzylamide were obtained from Aldrich.

Chromatographic Analysis. Sulfoxide derivatives were separated isocratically on a Waters HPLC and detected at

[†] This work was supported by United States Public Health Service Grant AA00279 (B.V.P.) and a predoctoral fellowship from The University of Iowa Center for Biocatalysis and Bioprocessing (H.C.).

[‡] The X-ray coordinates and structure factors have been deposited in the Brookhaven Protein Data Bank with entry names 1BTO and 3BTO, and r1btofs and r3btofs, respectively.

[§] The University of Iowa.

[||] Swedish University of Agricultural Sciences.

[⊗] Abstract published in *Advance ACS Abstracts,* December 15, 1996.

[1] Abbreviations: ADH, alcohol dehydrogenase; BTO, 3-butylthiolane 1-oxide; *P1*−*P4*, 3-butylthiolane 1-oxides eluted in peaks 1−4, respectively, on the Chiralcel OB-H column; HPLC, high-performance liquid chromatography; CD, circular dichroism; NMR, nuclear magnetic resonance; COSY, correlation spectroscopy; NOE, nuclear Overhauser effect; HMQC, heteronuclear correlation through multiple-bond coherence; Eu(hfc)$_3$, europium tris[3-[(heptafluoropropyl)hydroxymethylene]-(+)-camphorate]; NCS, noncrystallographic symmetry.

S0006-2960(96)02460-9 CCC: $14.00

214 nm using Cyclobond III (α-cyclodextrin, Rainin, 4.6 mm × 250 mm) and Chiralcel OB-H (Chiral Technologies Inc., 4.6 mm × 250 mm) columns developed with *n*-hexane/2-propanol or hexane/ethanol. The concentrated fractions were rechromatographed to confirm enantiomeric purity. The concentration of BTO was determined using UV spectrophotometry (ϵ_{210} in hexane = 2100 M^{-1} cm^{-1}, ϵ_{222} in water = 820 M^{-1} cm^{-1}).

Kinetic Studies. For kinetic studies, crystalline ADH was sedimented, solubilized in buffer, and dialyzed to remove ethanol. Inhibition of the forward reaction by mixed or separated stereoisomers was studied with varied concentrations of inhibitors against varied concentrations of ethanol (0.4−2 mM) with 1 mM NAD^+ in 46 mM sodium phosphate buffer at pH 7 and 25 °C. For inhibition studies of the reverse reaction, freshly distilled acetaldehyde (1−5 mM) and 0.1 mM NADH were used. The change of absorbance at 340 nm on a Cary 118C spectrophotometer was used to determine the initial velocities. Data were fitted to the equations for noncompetitive [$v = VA/[K_m(1 + I/K_{is}) + A(1 + I/K_{ii})]$] and uncompetitive [$v = VA/[K_m + A(1 + I/K_{ii})]$] inhibition (Cleland, 1979). The best fit was evaluated by comparison of the standard errors and variance.

Nuclear Magnetic Resonance. One-dimensional proton NMR, proton-decoupled, two-dimensional COSY, NOESY, and HMQC spectra were obtained using a Varian UNITY 500 pulsed Fourier transform spectrometer at 25 °C, except the spectra with 1 equiv of (*R*)-(−)-*N*-(3,5-dinitrobenzoyl)-α-methylbenzylamine were measured using a Bruker WM-360 MHz spectrometer. Samples were dissolved in $CDCl_3$ at a final concentration of several millimolar. Tetramethylsilane was used as an internal reference. For the NMR with the europium chiral shift reagent, the $Eu(hfc)_3$ concentration was increased stepwise in 0.01 equiv. NMR data were processed using a Varian NMR program.

Computational Modeling. Four stereoisomers of BTO were built and energy minimized (Powell method) using the computer program SYBYL (Tripos Associates). Cartesian coordinates of various possible conformations were obtained by dynamic simulation at 700 K for 1000 fs with annealing to 200 K for 1000 fs. Snapshots at every 50 fs of one 10-cycle simulation resulted in 500 coordinate sets. The Mulliken charge of each atom connected to the ring was calculated both by the semiempirical molecular orbital method (MOPAC program in SYBYL) and by the quantum-mechanical *ab initio* molecular orbital method (Gaussian program GAMESS; Schmidt et al., 1993). For *ab initio* charge calculation, the 6-31G basis set was used with PM3-optimized *Z*-matrix coordinates. Several differently ring-puckered conformations of each stereoisomer were docked into the active site of ADH, and torsion angles for the butyl group were adjusted using the program O (Jones et al., 1991) in order to obtain the starting model that best fit the electron density maps.

X-ray Crystallography. Crystals of the ternary complexes of ADH with NADH and stereoisomers of BTO were prepared by dialyzing about 1 mL of 10 mg/mL recrystallized horse liver enzyme against 10 mL of 50 mM ammonium *N*-[tris(hydroxymethyl)methyl]-2-aminoethanesulfonate buffer at pH 7 and 4 °C, with 0.66 mM NADH, 0.23 mM *P1* or 0.76 mM *P3*, and gradually increasing concentrations of 2-methyl-2,4-pentanediol. Crystals formed after addition of about 12% diol, and a final concentration of 25% was reached in 8 weeks. The crystals were flash-frozen at 100 K in a stream of N_2 without any additional cryoprotectant. Data were collected on an *R*-axis II image plate with a Rigaku rotating anode. Data were processed and scaled using the programs DENZO and SCALEPACK (Otwinowski, 1993) and converted to *F*'s using the program TRUNCATE in the CCP4 package (CCP4 Suite, 1994). The qualities of the final models were checked using the programs WHATIF and PROCHECK (Laskowski et al., 1993).

Table 1: X-ray Data and Refinement Statistics for Liver Alcohol Dehydrogenase Complexed with NADH and Isomers of 3-Butylthiolane 1-Oxide

	1*S*,3*R* isomer	1*S*,3*S* isomer	1*S*,3*S* isomer
subunits per asymmetric unit	4	2	4
total reflections measured	155 768	54 650	307 946
R_{merge} (%)[a]	4.3	8.1	5.3
unique reflections used	78 371	32 148	155 052
percent completeness	79	90	89.8
resolution range (Å)	20−2.1	20−2.3	20−1.66
R_{value}, R_{free} (%)[b]	19.0, 23.0 (3)	19.4, 24.7 (4)	18.1, 21.9 (1)
bond distances[c]	0.01	0.02	0.02
bond angles[c]	1.7	1.6	2.7
water molecules	1471	504	1616

[a] $R_{merge} = (\sum|I-\langle I\rangle|)/\sum\langle I\rangle$. [b] $R_{value} = (\sum|F_o-kF_c|)/\sum|F_o|)$, where *k* is a scale factor. The R_{free} values were calculated with the percentage of the reflections not used in the refinement indicated in parentheses. [c] Root-mean-square deviations (rmsd) from the ideal geometry of the final model.

The crystals for the complex with *P1* BTO (1*S*,3*R* isomer) belonged to the monoclinic space group $P2_1$ with the following dimensions: $a = 49.93$ Å, $b = 180.2$ Å, $c = 86.79$ Å, and $\beta = 106.0°$. Since the cell dimensions were significantly different from those of any previous crystal form of the horse liver enzyme, and there were two dimers in the asymmetric unit, the structure needed to be solved again. Molecular replacement using the program AMORE (Navaza, 1994) and the monomer of the refined horse liver structure (Ramaswamy et al., 1994) was used to obtain the starting model. Refinement was begun using the program XPLOR (Brünger et al., 1987), using rigid body refinement of the structure as a whole and then as dimers, as monomers, and as domains, which led to the NCS matrices. Data from 8.0 to 2.1 Å resolution were used for a cycle of positional, simulated annealing and temperature factor refinement, and the resulting coordinates were used to do a cycle of density modification and 4-fold averaging with DM (Cowtan, 1994). The maps were inspected using the program O (Jones et al., 1991) and clearly revealed the position of the NADH, a large number of waters, and the inhibitor. NADH and waters were added at this stage. After another round of refinement, several more waters and the inhibitor in the 1*S*,3*S* configuration were added, and the protein was refitted graphically. Another round of refinement with strict NCS led to an R_{value} of 22.6%, with an R_{free} of 24.8%. The modeled BTO remained in the 1*S*,3*S* configuration. At this stage, we used the program REFMAC (Murshadov et al., 1996), which uses the philosophy of maximum likelihood of phases for refinement. The following steps were done in cycles: run PROTIN to prepare restraints for the refinement, use REFMAC with strict NCS restraints on all atoms to refine, calculate maps and average them with RAVE (Kleywegt & Jones, 1996), use ARP (Lamzin & Wilson, 1993) to add or delete waters corresponding to one subunit, and generate all

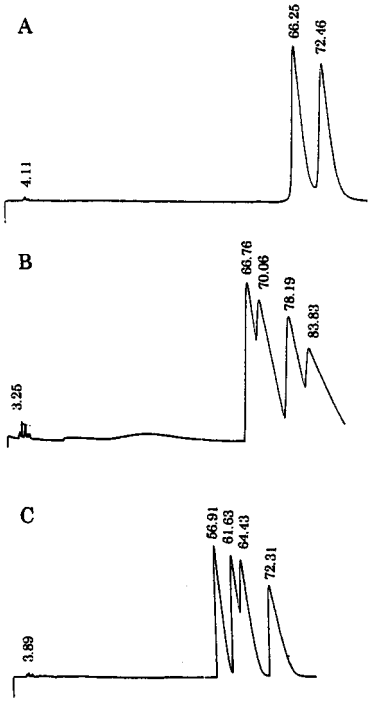

FIGURE 1: Chromatographic separation of the isomers of 3-butylthiolane 1-oxide. Detection was at A_{214}. The retention time was in minutes: (A) α-cyclodextrin column, developed with 90/10 v/v hexane/2-propanol at a flow rate of 0.6 mL/min with 1000 psi; (B) Chiralcel OB-H column, developed with 99.5:0.5 v/v *n*-hexane/2-propanol at a flow rate of 1.0 mL/min with 600 psi; and (C) Chiralcel OB-H column, developed with 99.5:0.5 v/v *n*-hexane/ethanol at a flow rate of 1.0 mL/min with 600 psi.

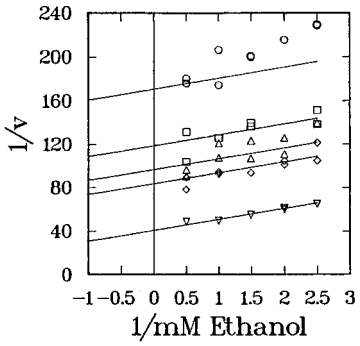

FIGURE 2: Inhibition of alcohol dehydrogenase by *P1* BTO (1*S*,3*R* isomer). Varied concentrations of *P1* (0, 0.33, 0.46, 0.6, and 1 μM; ▽, ◇, △, □, and ○, respectively) against varied concentrations of ethanol (0.4−2 mM) were used with 1 mM NAD^+ in 46 mM sodium phosphate and 0.25 mM EDTA buffer at pH 7 and 25 °C. Assays were in duplicate. Data were fitted with the program UNCOMP (Cleland, 1979).

four subunits. This was followed by several cycles of refinement with the same protocol, but applying tight NCS restraints only to the protein atoms and without averaging the maps, which led to an R_{value} of 19% and an R_{free} of 23%. The maps showed that only a few side chains of residues on the surface have uncertain or multiple positions. The Ramachandran plot indicated that only the four Cys-174 residues are not in "allowed regions". This residue is ligated to the catalytic zinc and is known to have a strained conformation (Ramaswamy et al., 1994). Table 1 summarizes the data and refinement.

A surprising outcome was that the refinement program (REFMAC) automatically changed the chirality of the modeled inhibitor from 1*S*,3*S* to 1*S*,3*R* in all four subunits.

Table 2: Inhibition Constants for Stereoisomers of 3-Butylthiolane 1-Oxides with Horse Liver Alcohol Dehydrogenase[a]

	BTO racemate	*P1* (1*S*,3*R*)	*P2* (1*R*,3*S*)	*P3* (1*S*,3*S*)	*P4* (1*R*,3*R*)
K_{ii} (μM)	0.56	0.31	37	0.72	7.3

[a] Inhibition studies were performed with varied concentrations of inhibitors against varied concentrations of ethanol (0.4−2 mM) at 1 mM NAD^+ in 46 mM sodium phosphate and 0.25 mM EDTA at pH 7 and 25 °C. The intercept inhibition constants, K_{ii}, were calculated from the fit for uncompetitive inhibition (Cleland, 1979). The standard errors were 4−8% of the values.

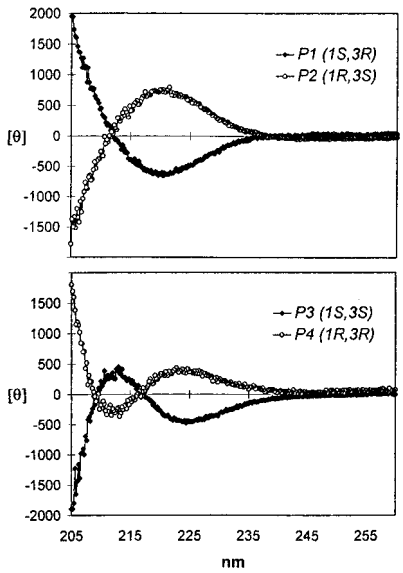

FIGURE 3: CD spectra of stereoisomers of BTO in water. The CD scans were carried out every 0.2 nm with an AVIV 62Ds CD spectometer at 25 °C. Background absorbance from the solvent was digitally subtracted. Molar ellipticity ([θ]) was calculated using the equation $[\theta] = 10\theta/dC$, where d is the path length in decimeters and C is the molar concentration.

The result was verified by starting again with either the *S*,*R* or *S*,*S* isomers, and in both cases, the refinement returned the *S*,*R* configuration. In contrast, a retrospective XPLOR refinement returned the input configuration.

Data were likewise collected from flash-frozen crystals of the complex with *P3* BTO (1*S*,3*S* isomer), but a crystal was found that belonged to the monoclinic space group $P2_1$ with the following dimensions: $a = 49.4$ Å, $b = 180.4$ Å, $c = 43.7$ Å, and $\beta = 107.8°$, which are very close to the cell dimensions of the monoclinic form found at 4 °C. The structure was refined by the same procedure described for *P1*. A 1.66 Å resolution data set was also collected at the BW7B beamline at the EMBL DESY, Hamburg, mounted with an MAR image plate. The crystals had the same cell dimensions as the complex with *P1*. Refinement started with the refined model for the complex with *P1* and proceeded by the same steps. In this case, the refinement retained the 1*S*,3*S* configuration.

RESULTS AND DISCUSSION

Separation of Stereoisomers. The chromatographic separation of the isomers of BTO is illustrated in Figure 1. BTO was separated into only two peaks on Cyclobond III (α-cyclodextrin) chiral phase. The four enantiomers were separated with moderate resolution on a Chiralcel OB-H (cellulose tribenzoate) column using 0.5% 2-propanol in

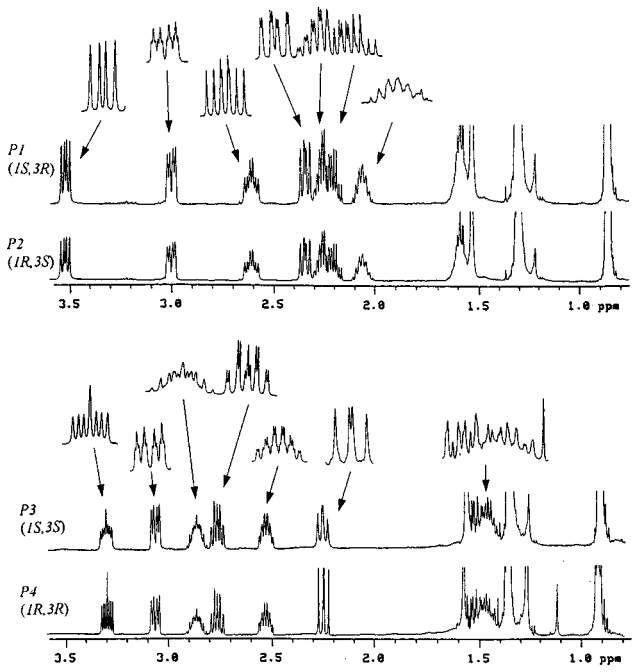

FIGURE 4: 500 MHz ^{1}H-NMR spectra of stereoisomers of BTO in $CDCl_3$, at 25 °C. The signals for protons attached to the ring carbons were expanded by 2−3-fold.

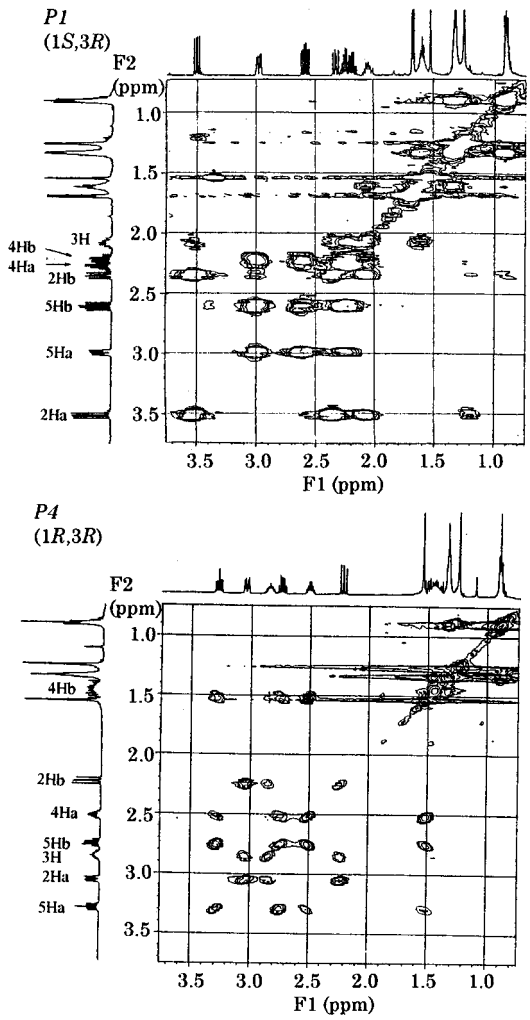

FIGURE 5: Two-dimensional COSY spectra and assigned carbon number based on cross-peaks. $CDCl_3$ was used as a solvent at 23 °C. The sample of *P1* contained the chiral shift reagent, (*R*)-(−)-*N*-(3,5-dinitrobenzoyl)-α-methylbenzylamine, and the spectrum had a shorter acquisition time than that of *P4*.

hexane or 0.5% ethanol in hexane. [The resolution on Chiralcel OD-H [cellulose tris(3,5-dimethylphenyl carbamate)] was not as good.] The order of separated peaks on the Chiralcel OB-H column under different conditions was the same even though the patterns were different. The area under each peak was as expected for the racemic mixture. Interestingly, the first peak from Cyclobond III corresponds to the third and fourth peak on Chiralcel OB-H. The four enantiomers were obtained in pure form by sequential separation on two columns, developed under different conditions.

Chiralcel OB-H is widely used for the separation of chiral sulfoxides. For phenylmethyl sulfoxide and alkyl *p*-tolyl sulfoxides, the (*S*)-(−) enantiomer elutes more rapidly than the (*R*)-(+) isomer using a solvent system of 2-propanol/hexane or ethanol/hexane (Colonna et al., 1992).

As will be demonstrated later, *P1* is the 1*S*,3*R* isomer, *P2* 1*R*,3*S*, *P3* 1*S*,3*S*, and *P4* 1*R*,3*R*. According to the crystallographic results, *P1* is the 1*S*,3*R* enantiomer, and *P3* has the 1*S*,3*S* configuration. Thus, both 1*S* enantiomers of BTO are eluted earlier than their 1*R* enantiomers on the Chiralcel OB-H column.

Inhibition Studies. The inhibition of ethanol oxidation by racemic BTO was best described as uncompetitive, with an intercept inhibition constant, K_{ii}, of 0.56 μM. Inhibition of the reduction of acetaldehyde was noncompetitive ($K_{is} = 0.65 \pm 0.07$ μM and $K_{ii} = 1.75 \pm 0.15$ μM). These results suggest that BTO binds preferentially to the enzyme−NADH complex and weakly to other forms of the enzyme, such as the enzyme−NAD^+ complex.

Each isomer of BTO also was uncompetitive against ethanol (Figure 2), but with very different inhibition constants (Table 2). 3-Substituted thiolane 1-oxides had higher affinities than tetramethylene sulfoxide itself ($K_{ii} = 19$ μM) because of the increased hydrophobic interaction in the extended substrate binding pocket and the side chain of the thiolane 1-oxides (Chadha et al., 1985). For the 1*R* isomers of BTO, however, the 3-butyl group did not increase the binding affinities as compared to that of unsubstituted tetramethylene sulfoxide. The 1*S*,3*R* and 1*S*,3*S* isomers had 100- and 10-fold lower K_{ii} inhibition constants (0.31 and 0.72 μM, respectively) than the 1*R*,3*S* and 1*R*,3*R* isomers (Table 2). These data indicate that the chirality and position of the butyl side chain have significant effects on binding affinities.

CD Spectroscopy and the Cotton Effect. The CD spectra (Figure 3) of *P1* and *P2* of BTO showed mirror symmetry, as did those of *P3* and *P4*. Thus, *P1* and *P2* is one enantiomeric pair, and *P3* and *P4* is the other.

The Cotton effect around λ_{max} of a functional group reflects the absolute configuration (Sandström, 1995). Cotton effects of ketone or exiton-coupled compounds have been intensively studied and can be applied to determine the configuration of chiral molecules (Lightner, 1994). However, it is difficult to predict the Cotton effects of sulfoxides. Mislow et al. (1965) observed positive Cotton effects for the alkyl *S*-sulfoxides. In hexane, λ_{max} of BTO is about 210 nm, but in water, λ_{max} is shifted to 222 nm. Positive Cotton effects were observed near the λ_{max} of *P2* and *P4*, which have the *R* configuration at sulfur. *P1* and *P3* had negative Cotton effects. Thus, the Cotton effects of the stereoisomers of BTO are opposite to those of the linear sulfoxides and reflect the overall structures.

NMR Studies. ^{1}H-NMR spectra (Figure 4) also showed that *P1* and *P2* is one enantiomeric pair and *P3* and *P4* the

Table 3: Assigned Proton Chemical Shifts and Coupling Constants for Isomers of 3-Butylthiolane 1-Oxides[a]

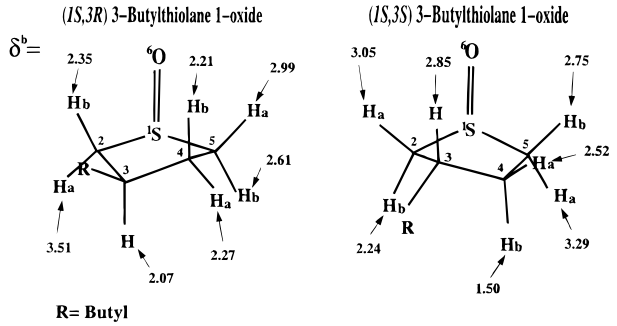

		P1 (1*S*,3*R*)	*P4* (1*R*,3*R*)
$^2J_{gem}$	$J_{2H_a-2H_b}$	13.9	13.7
	$J_{4H_a-4H_b}$	12.8	13.0
	$J_{5H_a-5H_b}$	13.6	14.0
$^3J_{vic}$	J_{2H_a-3H}	8.3	5.9
	J_{2H_b-3H}	9.0	11.1
	J_{4H_a-3H}	ND[c]	6.0
	J_{4H_b-3H}	ND	ND
	$J_{4H_a-5H_a}$	2.1	4.6
	$J_{4H_a-5H_b}$	6.3	8.0
	$J_{4H_b-5H_a}$	5.8	9.1
	$J_{4H_b-5H_b}$	12.4	ND
^4J	$J_{2H_a-5H_b}$	—[d]	1.6
	$J_{2H_b-5H_a}$	1.6	—
	$J_{2H_a-4H_a}$	—	1.6
	$J_{2H_b-4H_b}$	ND	—

[a] Coupling constants were identified through two series of decoupling experiments. Each time, one proton signal was irradiated at 90 °C and the difference of splitting from the reference spectrum was observed. [b] δ is defined as the center of a proton signal. R = a butyl group. [2] $^2J_{gem}$ is the two-bond *geminal* coupling constant. [3] $^3J_{vic}$ is the three-bond *vicinal* coupling constant. [4] ^4J is the four-bond coupling constant. [c] Not determined because of the complexity of splitting. [d] No coupling observed.

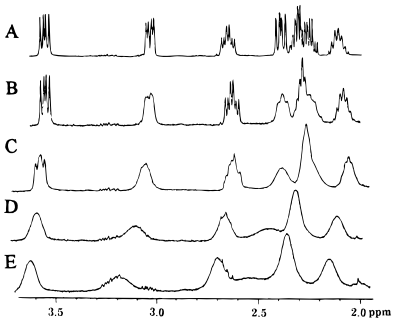

FIGURE 6: Induced chemical shifts and band broadening in the ^{1}H-NMR spectrum of *P2* upon addition of Eu(hfc)$_3$: (A) *P2* spectra without Eu(hfc)$_3$ and with (B) 0.005 equiv, (C) 0.01 equiv, (D) 0.02 equiv, and (E) 0.03 equiv of Eu(hfc)$_3$, respectively.

other. Assignment of the proton chemical shifts was an especially interesting problem. One might expect that the deshielding effect of the sulfoxide oxygen would be larger than that of the lone pair of electrons. However, the chemical shifts of protons in the α position of a sulfoxide are very sensitive to the solvent and the whole structure of the molecule (Lett & Marquet, 1971). We arbitrarily named protons bound to the same carbon as H_a and H_b, where H_a designates the proton located more downfield than H_b. The assignment to carbon number was established through the connectivity of the COSY spectra (Figure 5). Resonance frequency assignments of protons attached to the ring carbons deduced from the COSY spectrum of *P4* were consistent

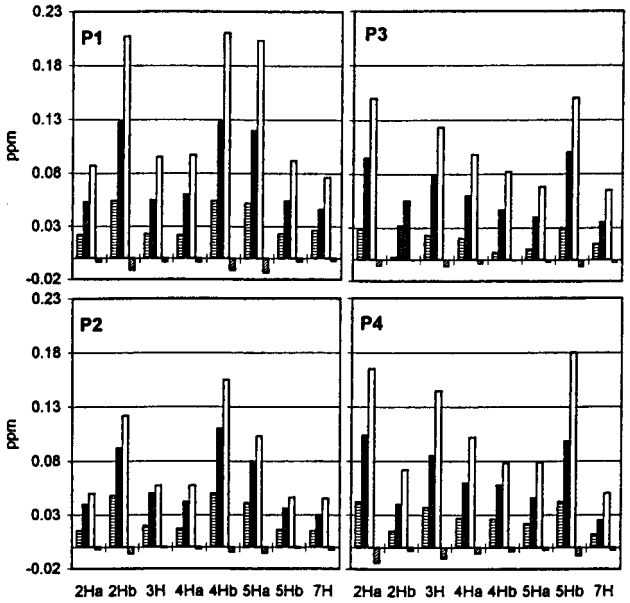

FIGURE 7: Pattern of induced $\Delta\delta$ upon addition of chiral shift reagents. Eu(hfc)$_3$ [0.01 equiv (hatched column), 0.02 equiv (closed column), and 0.03 equiv (open column)] and (*R*)-(−)-*N*-(3,5-dinitrobenzoyl)-α-methylbenzylamine [1 equiv (cross-hatched column)) were added to BTO stereoisomers.

with those obtained from the HMQC spectrum and with decoupling experiments (data not shown). Decoupling of ^{1}H-NMR for *P1* showed that $2H_a$ and $5H_b$ are coupled to each other. For *P4*, $2H_b$ and $5H_a$ are coupled to each other. These results are consistent with these closely coupled hydrogens being either *syn* to the S=O or *anti*; as it turned out, these hydrogens are *anti*.

In principle, the conformations and diastereomeric configurations could be established from the coupling constants. The coupling constants of NMR resonances for *P4* (Table 3) showed that θ (dihedral angle) between $2H_b$ and 3H is closer to 0 or 180° than θ is between $2H_a$ and 3H (based on Karplus relationship), since the $2H_b$ signal has a larger vicinal coupling constant ($^3J_{2H_b-3H}$ = 11 Hz) than the $2H_a$ signal ($^3J_{2H_a-3H}$ = 6 Hz). For a five-membered ring, however, the relationship between coupling constants and the dihedral angle would deviate from the standard Karplus relationship, and we could not confidently deduce θ values between ring hydrogens from the coupling constants.

We also tried to compute the average interproton distances from a series of NOE experiments with four different mixing times: 0.035, 0.095, 0.257, and 0.700 s. The NOE values (volume at zero mixing time) were obtained by extrapolation of the peak volume versus mixing time. The average interproton distance is computed from the relation that the ratio of NOE values is proportional to the ratio of the inverse of the sixth power of the distance. However, cross-peaks of NOESY spectra of *P4* showed uncommon shapes, a complex mixture of positive and negative peaks, in short mixing times (e.g., 0.035, 0.095, and 0.275 s). Thus, the calculation of the volume of cross-peaks was very difficult, and the average interproton distances computed from the cross-peak volume were not reliable.

Chiral shift reagents can be used to establish configuration if the reagent forms a defined complex with the compound. The oxygen atom of the sulfoxide moiety can make a hydrogen bond with (*R*)-(−)-*N*-(3,5-dinitrobenzoyl)-α-methylbenzylamine (Pirkle et al., 1982) and a coordinate bond

Table 4: Computed Mulliken Charges on Sulfoxide and Protons Attached to the Thiolane 1-Oxide Ring Carbons[a]

	charge on (1*S*,3*S*)-BTO			charge on (1*S*,3*R*)-BTO		
	MNDO	PM3	RHF/6-31G[d]	MNDO	PM3	RHF/6-31G[d]
1S	0.953	0.949	0.897	0.954	0.948	0.886
6O	−0.728	−0.674	−0.781	−0.728	−0.673	−0.774
$2H_{syn}$[b]	0.104	0.185	0.247	0.105	0.187	0.245
$2H_{anti}$[c]	0.076	0.174	0.202	0.075	0.167	0.203
3H	0.068	0.150	0.207	0.052	0.136	0.178
$4H_{syn}$	0.060	0.138	0.218	0.062	0.143	0.216
$4H_{anti}$	0.051	0.130	0.181	0.051	0.126	0.180
$5H_{syn}$	0.106	0.106	0.243	0.107	0.183	0.242
$5H_{anti}$	0.077	0.077	0.198	0.076	0.165	0.200

[a] The program SYBYL, with routines MNDO and PM3, was used for semiempirical calculation. GAMESS was used for the quantum-mechanical method, Gaussian calculation with RHF/6-31G basis set and Runtype set to Gradient (Schmidt et al., 1993). [b] *Syn* position to sulfoxide oxygen. [c] *Anti* position to sulfoxide oxygen. [d] 3-Methylthiolane 1-oxide was used instead of 3-butylthiolane 1-oxide to decrease the run time and memory requirements.

with the europium of the lanthanide shift reagent (Cockerill et al., 1973). Europium, like other rare earth ions, is known to make 8-fold or more coordination because of a large ionic radius and the availability of vacant orbitals to accommodate electron pairs donated by Lewis bases (Brecher et al., 1965). Therefore, the protons near the sulfoxide oxygen should be affected more than distant protons (Shapiro et al., 1971). Addition of $Eu(hfc)_3$ resulted in band broadening and induced shifts (Figure 6). More shifted protons showed more severe band broadening. One-dimensional-NMR of *P1* and *P2* showed that adding either (*R*)-(−)-*N*-(3,5-dinitrobenzoyl)-α-methylbenzylamine or $Eu(hfc)_3$ affected the $2H_b$, $4H_b$, and $5H_a$ signals more than the $2H_a$, 3H, $4H_a$, and $5H_b$ signals (Figure 7). For *P3* and *P4*, $2H_a$, 3H, $4H_a$, and $5H_b$ signals shifted more than the $2H_b$, $4H_b$, and $5H_a$ signals. These chiral shift reagent data indicate that the chemical shift patterns of the two diastereoisomers are opposite with respect to each other, which are consistent with the data from the decoupling experiments. $2H_b$, $4H_b$, and $5H_a$ of *P1* and *P2* are the protons *syn* to S═O, whereas $2H_a$, $4H_a$, and $5H_b$ of *P3* and *P4* are *syn* to S═O (Table 3). These results show again that the chemical shifts of protons in sulfoxide compounds are very sensitive to the structure of the molecule and not obviously predictable.

In determination of the absolute configuration of sulfoxide compounds using NMR, the most critical issue is whether the deshielding effect of the sulfoxide oxygen is larger than that of the unshared pair of electrons. Biotin sulfoxide and penicillin *S*-oxide are the most extensively studied sulfoxides. Harrison and Hodge (1976) and Kemp et al. (1979) determined the chemical shift values (δ) of various derivatives of penicillin and cephalosporin. In their studies, 5H of the α-sulfoxide (*syn* to sulfoxide oxygen) has a smaller δ than 5H of the β sulfoxide (*anti* to sulfoxide oxygen). However, the β-lactam has nitrogen and a carbonyl group in the fused ring and a carboxyl substituent at C3. Biotin also has a fused ring with two nitrogens and a carbonyl functional group, but not adjacent to the sulfoxide. Thus, it is more similar to thiolane 1-oxide. On the basis of the J_{gem} relation of biotin sulfoxide, Liu and Leonard (1979) concluded that the 4H (*syn* to oxygen) signal of the α-sulfoxide is more downfield than the 4H signal of the β-sulfoxide. Thus, the decoupling studies and the NMR with the chiral shift reagent demonstrate that the pattern of actual chemical shifts of the protons adjacent to S═O in BTO is complex and could not be predicted from previous studies.

Molecular Modeling and Quantum-Chemical Calculation. Table 4 shows that all the protons *syn* to the sulfoxide oxygen of the stereoisomers of 3-substituted thiolane 1-oxide have more positive charge (less electron density) than the corresponding *anti* protons, regardless of calculation methods. Because the variation in electron density around a proton is the most important factor influencing its chemical shift, these calculations support the proposal that *syn* protons might be more deshielded than *anti* protons. The charge on 3H of the *S*,*S* isomer is significantly higher than that of the *S*,*R* isomer. The chemical shift of 3H is 2.08 ppm in *P1* and 2.85 ppm in *P4*. Therefore, *P1* would correspond to either the *R*,*S* or *S*,*R* configuration on the basis of calculated charges of 3H, even though the deshielding effect of the sulfoxide oxygen or unpaired electrons on 3H might be much smaller than that for 2H or 5H, through both bonds and space. However, the calculated electron density could not predict the relative chemical shifts of 2H and 5H consistently. The chemical shifts of protons attached to the ring are determined by the overall conformation and sum of shielding or deshielding effects of the induced magnetic field due to the 3-butyl and sulfoxide groups.

Structures of Ternary Complexes. The electron density maps of the ternary complexes of enzyme and NADH with the BTO isomers in *P1* or *P3* clearly showed that sulfurs have the *S* configuration (Figure 8). Both the 1*S*,3*R* and 1*S*,3*S* isomers appeared to fit quite well to the 2.1 Å electron density map of the enzyme−NADH−*P1* complex. However, refinement showed that *P1* was the 1*S*,3*R* isomer. The distance between sulfoxide oxygen and the zinc atom in active site is about 2.2 Å. Tables 5 and 6 and Figure 8C show that the binding modes for 1*S*,3*R* and 1*S*,3*S* isomers are different. The butyl group of the 1*S*,3*R* isomer points toward Leu-309 and Met-306 of the other subunit (labeled L709 and M706), whereas the butyl group of the 1*S*,3*S* isomer points to Leu-116. Furthermore, the side chains of Leu-116, Ile-318, and Met-306 (M706) and Leu-309 (L709) of the adjoining subunit have different rotamer conformations in the complexes with the different isomers.

The structures of the protein moieties in the two different complexes studied at 100 K are very similar to the structure of the enzyme complexed with NAD^+ and pentafluorobenzyl alcohol studied at 278 K (Ramaswamy et al., 1994). All have the "closed" conformation. The Cα atoms of the subunits of the enzymes complexed with the sulfoxides can be superimposed on the subunits of the enzyme complexed with NAD^+ with pentafluorobenzyl alcohol with average rms differences of 0.27 Å. The small differences appear in loops containing residues 33, 57, 134, and 246. The four subunits in the asymmetric units of the complexes with the 1*S*,3*R*

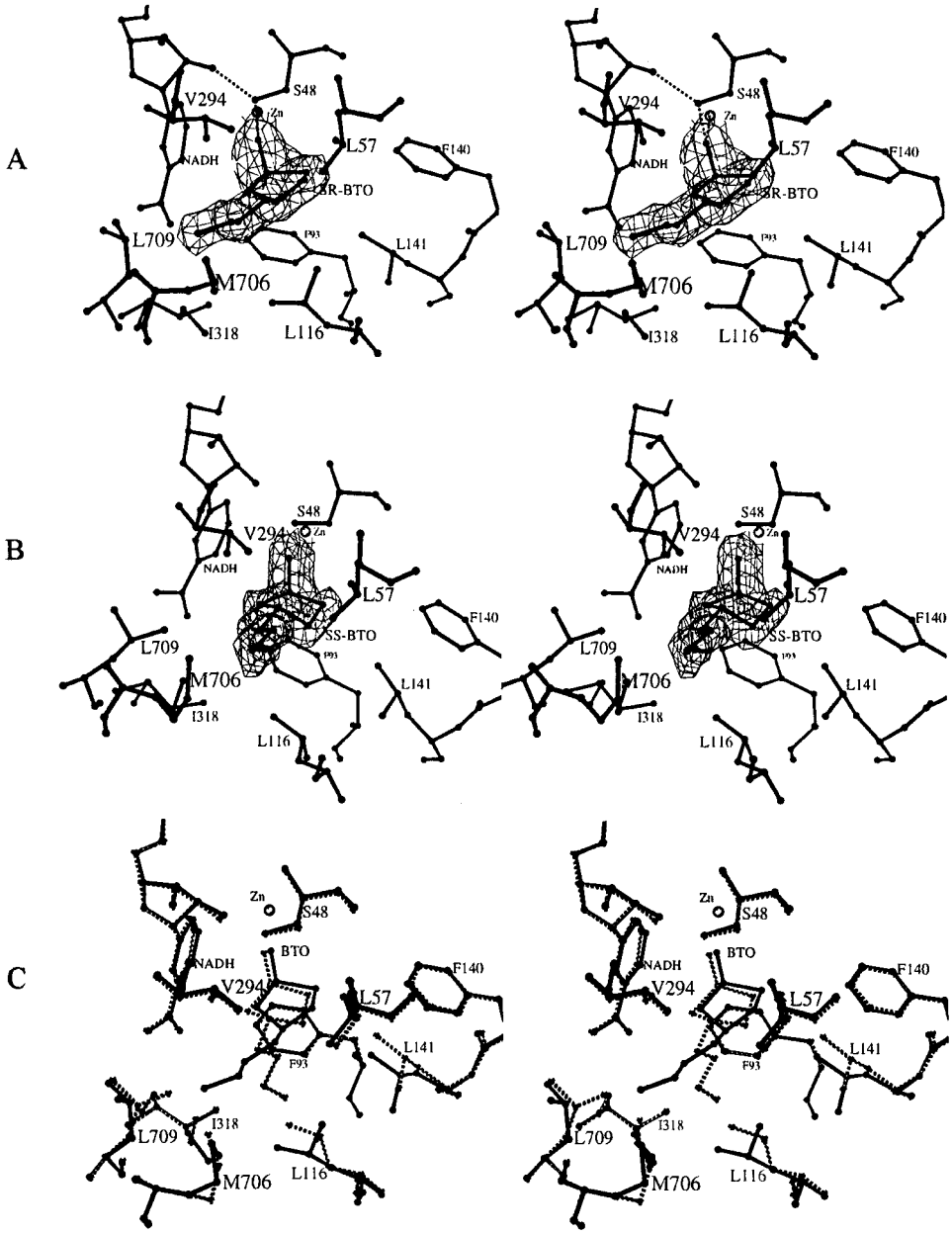

FIGURE 8: Electron density maps and the fitted structures for 3-butylthiolane 1-oxides binding to the alcohol dehydrogenase−NADH complexes: (A) (1*S*,3*R*)-BTO binding in the enzyme−NADH−*P1* complex, (B) (1*S*,3*S*)-BTO binding in the enzyme−NADH−*P3* complex, and (C) comparison of binding modes with the structure for the 1*S*,3*S* isomer shown in dashed lines. The figures were prepared with MOLSCRIPT (Kraulis, 1991).

and 1*S*,3*S* isomers are also very similar, as the rms differences in the Cα positions are 0.08 or 0.09 Å, respectively. The structures of the subunits of the complexes with the 1*S*,3*S* isomers in the two different unit cells are also similar (rmsd of 0.16 Å). The different packing of subunits in the complexes with NADH and the sulfoxides does not appear to significantly affect the tertiary structures.

The most tightly bound stereoisomer might resemble the transition state for hydrogen transfer (Wolfenden, 1972; Tapia et al., 1988). However, the sulfoxides appear to be rotated about 90° from a position where a hydride ion could be transferred directly from NADH. Interestingly, the sulfur interacts with the benzene ring of Phe-93, in what may be considered to be a "cation−π" interaction (Dougherty, 1994). The charge on the sulfur, as calculated with SYBYL and GAMESS, is about +0.9, and the charge on the oxygen is about −0.7. The distance from the positively charged sulfur to the center of the electron-rich π ring is about 3.4 Å, which is close enough to stabilize the binding. This cation−π interaction appears to be important in the determination of the binding mode of the sulfoxide inhibitors. The structure of the complex with dimethyl sulfoxide has an almost identical geometry (Al-Karadaghi et al., 1994). These structures provide a basis for modeling the binding of other inhibitors and reaction intermediates.

ACKNOWLEDGMENT

We thank Dr. William R. Kearney in the College of Medicine NMR Facility, The University of Iowa, for his advice on NMR studies; Björn Kauppi for help in data collection; and Prof. Hans Eklund of the Department of Molecular Biology, Swedish University of Agricultural Sciences, for advice and support.

Table 5: X-ray Crystallographic Analysis of Flexibility in Binding[a]

		torsion angles of side chains	
		E−NADH−(*S*,*R*)-BTO	E−NADH−(*S*,*S*)-BTO
BTO	$\alpha_{C2-C3-C7-C8}$	59	−175
	$\beta_{C3-C7-C8-C9}$	177	170
	$\gamma_{C7-C8-C9-C10}$	164	177
Leu-57	χ^1	−174	−178
	χ^2	55	54[b]
Leu-116	χ^1	176	−84
	χ^2	65	100
Leu-141	χ^1	−66	−51
	χ^2	173	178
Ile-318	χ^1	−69	−60
	χ^2	160	−63
Met-306[c]	χ^1	−135	−172
	χ^2	32	68
	χ^3	−115	22
Leu-309[c]	χ^1	−104	−160
	χ^2	−26	75

[a] The torsion angles in all four subunits are about same (within ±5°). The electron densities for the side chains are usually very well-defined, and the temperature factors are comparable to those for other atoms in the molecules. For the complex with the *S*,*R* isomer, the average temperature factor for the whole molecule was 16.9 ± 6.3. In the complex with the *S*,*S* isomer, the average temperature factor was 14.1 ± 5.5, and all residues had factors within this range, except Leu-116, which averaged 21. [b] Leu-57 of subunit C has a different value for χ^2 of 174, and the electron density suggests alternate conformations in all four subunits. [c] These residues belong to the other subunit of the dimer.

Table 6: Comparison of Binding of Sulfoxides in the Enzyme-NADH Complexes

		interaction distances (Å)[a]		
		1*S*,3*R*	1*S*,3*S*	Me_2SO[b]
Cat Zn	Cys-46 SG	2.2	2.2	2.2
Cat Zn	Cys-174 SG	2.2	2.3	2.3
Cat Zn	His-67 NE2	2.2	2.1	2.1
O	Cat Zn	2.3	2.2	2.2
O	C5 of NADH	3.2	3.2	3.3
O	Ser-48 OG	2.6	2.6	2.6
O2′ of NADH	Ser-48 OG	2.6	2.7	2.8
O2′ of NADH	His-51 NE2	3.1	3.1	3.0
O3′ of NADH	His-51 NE2	3.0	3.0	3.1
S	Phe-93 CZ	3.4	3.4	3.5
S	C4 of NADH	3.7	3.6	3.8
C2	Phe-93 CE1	3.7	3.8	3.7
C2	O7N of NADH	3.7	3.4	3.8
C5	Leu-141 CD1	3.5	3.4	3.5
C5	Ser-48 CB	3.8	3.7	3.6
C5	Phe-140 CZ	4.3	4.8	4.6
C5	His-67 CD2	3.3	3.7	3.9

[a] Distances are averages over the subunits and have ranges of ± 0.1 Å. [b] Structure with dimethyl sulfoxide (Al-Karadaghi et al., 1994), with carbon 2 arbitrarily relabeled as C5.

REFERENCES

Al-Karadaghi, S., Cedergren-Zeppezauer, E., Hövmoller, S., Petratos, K., Terry, H., & Wilson, K. S. (1994) *Acta Crystallogr. D50*, 793−807.

Blomstrand, R., Östling-Wintzell, H., & Löf, A. (1980) *Arch. Biochem. Biophys. 199*, 591−605.

Brecher, C., Samelson, H., & Lempicki, A. (1965) *J. Chem. Phys. 42*, 1081−1096.

Brünger, T. A., Kuriyan, J., & Karplus, M. (1987) *Science 235*, 458−460.

CCP4 Suite (1994) *Acta Crystallogr. D50*, 760−763.

Chadha, V. K., Leidal, K. G., & Plapp, B. V. (1983) *J. Med. Chem. 26*, 916−922.

Chadha, V. K., Leidal, K. G., & Plapp, B. V. (1985) *J. Med. Chem. 28*, 36−40.

Chen, W.-S., Bolhken, D. P., & Plapp, B. V. (1981) *J. Med. Chem. 24*, 190−193.

Cleland, W. W. (1979) *Methods Enzymol. 63*, 103−138.

Cockerill, A. F., Davies, G. L. O., Harden, R. C., & Rackham, D. M. (1973) *Chem. Rev. 73*, 553−588.

Colonna, S., Gaggero, N., Casella, L., Carrea, G., & Pasta, P. (1992) *Tetrahedron: Asymmetry 3*, 95−106.

Cowtan, K. (1994) *Joint CCP4 and ESF-EACBM Newsletter on Protein Crystallography 31*, 34−38.

Dougherty, D. A. (1994) *Science 271*, 163−168.

Harrison, C. R., & Hodge, R. (1976) *J. Chem. Soc., Perkin Trans. 1*, 1972−1975.

Jones, T. A., Zou, J. Y., Cowan, S. W., & Kjeldgaard, M. (1991) *Acta Crystallogr. A47*, 110−119.

Kemp, J. E. G., Closier, M. D., & Stefaniak, M. H. (1979) *Tetrahedron Lett.*, 3785−3788.

Kleywegt, G. J., & Jones, T. A. (1996) *Acta Crystallogr. D52*, 826−828.

Kraulis, D. (1991) *J. Appl. Crystallogr. 24*, 946−950.

Laskowski, R. A., MacArthur, M. W., Moss, D. S., & Thornton, J. M. (1993) *J. Appl. Crystallogr. 26*, 286−290.

Lamzin, V. S., & Wilson, K. S. (1993) *Acta Crystallogr. D49*, 129−147.

Lett, R., & Marquet, A. (1971) *Tetrahedron Lett.*, 2855−2858.

Lightner, D. A. (1994) in *Analytical Applications of Circular Dichroism* (Purdie, N., & Brittain, H. G., Eds.) pp 131−174, Elsevier Science, Amsterdam, The Netherlands.

Liu, F.-T., & Leonard, N. J. (1979) *J. Am. Chem. Soc. 101*, 996−1005.

Mislow, K., Green, M. M., Laur, P., Melillo, J. T., Simmons, T., & Ternay, A. L., Jr. (1965) *J. Am. Chem. Soc. 87*, 1958−1976.

Murshadov, C., Vagin, A., & Dodson, E. (1996) in *Refinement of Protein Structures. Proceedings of the CCP4 Study Weekend*, SERC Daresbury Laboratory, Warrington, U.K.

Navaza, J. (1994) *Acta Crystallogr. 50*, 157−163.

Otwinowski, Z. (1993) in *Proceedings of the CCP4 Study Weekend* (Sawyer, L., Issacs, N., & Bailey, S., Eds.) pp 56−62, SERC Daresbury Laboratory, Warrington, U.K.

Pirkle, W. H., Finn, J. M., Hamper, B. C., Schreiner, J., & Pribish, J. R. (1982) *ACS Symp. Ser. 85*, 245−260.

Plapp, B. V. (1975) in *Biochemical Pharmacology of Ethanol* (Majchrowicz, E., Ed.) pp 77−109, Plenum, New York.

Plapp, B. V. (1994) in *Toward a Molecular Basis of Alcohol Use and Abuse* (Jansson, B., Jörnvall, H., Rydberg, U., Terenius, L., & Vallee, B. L., Eds.) pp 311−322, Birkhäuser Verlag, Basel, Switzerland.

Plapp, B. V., Leidal, K. G., Smith, R. K., & Murch, B. P. (1984) *Arch. Biochem. Biophys. 230*, 30−38.

Ramaswamy, S., Eklund, H., & Plapp, B. V. (1994) *Biochemistry 33*, 5230−5237.

Sandström, J. (1995) *Chirality 7*, 181−192.

Schmidt, M. W., Baldridge, K. K., Boatz, J. A., Elbert, S. T., Gordon, M. S., Jensen, J. H., Koseki, S., Matsunaga, N., Nguyen, K. A., Su, S., Windus, T. L., Dupuis, M., & Montgomery, J. A., Jr. (1993) *J. Comput. Chem. 14*, 1347−1363.

Shapiro, B. L., Hlubucek, J. R., Sullivan, G. R., & Johnson, L. F. (1971) *J. Am. Chem. Soc. 93*, 3281−3283.

Tapia, O., Cardenas, J. A., & Colonna-Cesari, F. (1988) *J. Am. Chem. Soc. 110*, 4046−4047.

Theorell, H., Chance, B., Yonetani, T., & Oshino, N. (1972) *Arch. Biochem. Biophys. 150*, 434−444.

Wolfenden, R. (1972) *Acc. Chem. Res. 5*, 10−18.

BI9624604